THE DEVELOPMENT OF A SCIENTIFIC PERMANENT SCATTERER SYSTEM

Nico Adam[a], Bert Kampes[a], Michael Eineder[a],
Jirathana Worawattanamateekul[b] and Michaela Kircher[b]

[a] DLR Oberpfaffenhofen, Remote Sensing Technology Institute (IMF), 82234 Wessling, Germany - Nico.Adam@dlr.de
[b] DLR Oberpfaffenhofen, German Remote Sensing Data Center, 82234 Wessling, Germany

KEY WORDS: Permanent Scatterer Interferometry, InSAR, D-InSAR

ABSTRACT:

DLR has achieved many years' experience concerning space born radar interferometry. The interferometric system *GENESIS* was improved and extended for different projects, e.g. for differential interferometry (D-InSAR) and for highly specialised missions as the Shuttle Radar Topography Mission (SRTM). Recently, a POLIMI researcher team invented the permanent scatterer technique and demonstrated the capability to monitor displacements in urban areas with millimetre accuracy. This new processing allows innovative data products and permits completely new geophysical applications. Consequently, DLR's interferometry system is extended also for this new processing technique. The implemented processing system is currently at the stage of a scientific development and research platform. The development from a scientific via a semi-operational and finally into an operational system is ongoing. In this paper the developed permanent scatterer system is presented and examples are shown for processing products as displacement maps, evolution in time of single scatterers, atmospheric phase screen, digital elevation model (DEM) updates, super resolution images, calibrated radar scenes and radiometric improved images. Moreover, results from current projects are presented.

1. INTRODUCTION

The permanent scatterer (PS) technique, invented at the POLIMI insititute (Ferretti et al., 2000a), is able to detect and monitor displacements in urban areas with millimetre accuracy per year. The existing limits of the InSAR technique are mastered by restriction of the estimation to point scatterers with long-term stable backscattering, extremely good signal-to-noise-ratio and also by the generation of a data series covering a long time span (Ferretti et al., 1999a).

In spite of our long-term experience developing radar interferometry software we consider the development of this scientific PS system as a new challenge. The operational DLR interferometry system GENESIS was a good starting point because its design is prepared for operational mass data processing (Eineder et al., 1997) like for the shuttle radar topography mission (SRTM).

The newly developed PS system has been influenced by the research of the POLIMI institute (Ferretti et al., 1999b, 2000b-e, 2001). Nevertheless, it is our aim to establish our own optimised general system concerning accuracy and easy usage. Many adaptations are necessary to the existing InSAR software: not only the amount of data to process has increased a lot but also the accuracy of many parameters has to be improved. Single algorithms that had been used successfully so far are to be made more robust and new modules like oversampling, signal-to-clutter-ratio (SCR) estimation and point target analysis have to be developed.

The first part of this paper provides an overview on the developed PS system. Thereafter, one of the most important algorithms, the coregistration, is described in more detail. Many data products are the result of the PS processing. In the third part some examples are be given for illustration, e.g. displacement maps, evolution in time of single scatterers, atmospheric phase screen (APS), digital elevation model (DEM) updates, super resolution images, calibrated radar scenes, radiometricaly improved images and visualisations. In the last section results from current application projects are presented.

2. SYSTEM OVERVIEW

The permanent scatterer technique needs to deal with a huge amount of data. Typically, a data stack consists of 60-100 single look complex (SLC) scenes. DLR-IMF's developed processing system is able to cope with this requirement and runs on high performance multi CPU and standard SUN workstations as well as on Linux PCs. Many software modules take advantage of multiple CPU computers by supporting multi-threading.

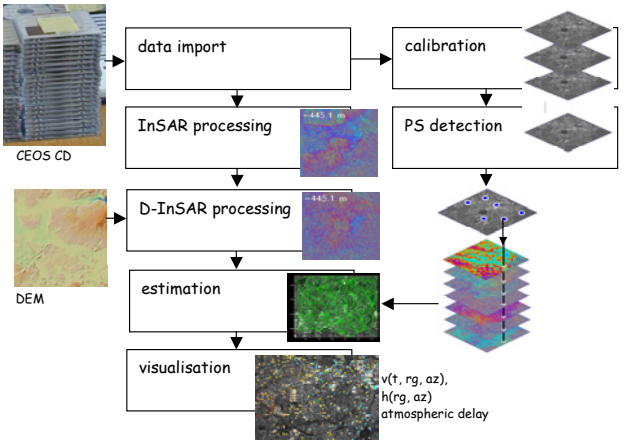

Figure 1. The structure of the overall PS system. Each box illustrates a sub-processing system.

Figure 1 shows the structure of the overall system. The present GENESIS system corresponds to the InSAR box. All the other sub-systems are extensions. The individual sub-systems use the data of the previous processing steps but work independently from each other. This means e.g. that we do not need new InSAR, D-InSAR or calibration processing for a test or a re-processing of the estimation. New SLC scenes can be integrated into the data stack without the current data being re-processed. Only the PS detection and the estimation itself should run anew because both processing steps take advantage of a new sample in the time series. The data dependencies and processing status

are checked automatically during processing. The newly developed permanent scatterer system is based on a modular concept. New algorithms can easily be plugged into the processing chain. Consequently, the accuracy of the algorithms can be assessed and they can be compared regarding their performance and robustness.

2.1 Data Input

This first processing step starts the initial data setup. When importing the first scene, the area of interest is selected graphically. The area typically is restricted to an urban area. Its geographical coordinates are used during the import of the following scenes to automatically extract the test site. In the meantime the SLC data are oversampled by zero padding by a factor of two because of the spectral conditions for the generation of the interferograms and a higher accuracy with the co-registration. Nutricato et al. (2002) have shown that also the PS identification takes advantage of this oversampling.

2.2 InSAR Processing

First, the master scene is selected in order to start the InSAR processing. Parameters as the effective baseline, the acquisition date, the Doppler centroid frequency and the season of the acquisition form the selection criteria. If the analysis indicates a strong atmospheric signal in the master scene the data stack can be easily re-processed with another master scene. During the InSAR processing the observation geometry parameters as the height-to-phase conversion factor, the flat-earth phase, the range distances and the look angle are computed. Furthermore, the scenes are co-registered and resampled with respect to the master scene and the interferograms are generated. Because of the utilisation of point scatterers, a spectral shift filtering is not necessary. Compared to the processing of short time span Tandem interferograms some processing steps are more difficult with the PS technique, e.g. the requirements concerning robustness and accuracy in co-registration as well as the requirements regarding the parameters for the observation geometry. The adaptation in both algorithms are described in section three.

2.3 D-InSAR Processing

During the differential interferometric processing step the observation geometry of the radar acquisition is simulated. A DEM and precise orbits are used as input. That means that the interferometric phase can be modelled. This module has been optimised for speed because many scenes are to be processed.
The range distances calculated during this processing step correspond to the range SLC and the azimuth times correspond to the azimuth SLC coordinates. Depending whether the master or the slave orbit is taken as the reference the slant range coordinates of the master or of the slave scene result. The relation between the two independent coordinate systems is provided by the common observation raster on the Earth's surface. Consequently, this module also determines the co-registration and is therefore also used for that processing step.

2.4 Calibration

The calibration of the scenes has been introduced for the PS detection. To analyse the temporal backscattering behaviour of the point scatterers it is necessary to compare their intensity. The SLC scenes have been acquired with different sensors like ERS-1 and ERS-2 or have been focused with different processing systems (D-PAF, I-PAF, UK-PAF). The developed module corrects for the processor gain constant, the antenna pattern and the range spreading loss. It calculates the radar cross section per unit area σ^0 (Laur et al., 2002):

$$\sigma^0 = \frac{\langle I \rangle}{K} \cdot \frac{\sin(\alpha)}{\sin(\alpha_{ref})} \cdot \frac{R^3}{R_{ref}^3} \cdot \frac{1}{g^2(\theta)} \cdot \qquad (1)$$

Some of the SLC scenes have been focused with a nominal chirp depending on the processing system and of the status of the ERS sensors. These scenes are calibrated with the most recent sensor calibration parameters (Meadows et al., 2001).
Alternatively to the implemented absolute calibration a relative calibration (Bovenga et al., 2002) is possible. But the implemented absolute calibration has the advantage that the measurement reflects a physical property of the scatterer. Consequently, the equivalent size of a corner reflector can be derived.

2.5 Permanent Scatterer Detection

The temporal analysis of the differential phases is restricted to point scatterers with a high SNR and a long-time stable backscattering behaviour. These are usually man-made features (Usai et al., 1999) and have to be detected in the scene. The PS identification is performed in the co-registered calibrated scenes by a homogeneity test (Ferretti et al., 2001). It is our aim to find as many scatterers as possible because a subsidence pattern and the atmosphere have to be sampled spatially as dense as possible. On the other hand, we want to avoid unreliable points causing incorrect estimation. The result is the phase information on an irregular grid. The extraction of the PS information reduces the amount of data from more than 100 GB to less than 300 MB. Range and azimuth position of the scatterer in the scene, the calibrated intensity, the look angle, the Doppler centroid frequency, the height-to-phase conversion factor, the temporal baseline, the scatterer subpixel position and the differential phase in a compact form are the result from this processing step. This processing step can be considered converting the raster data into vector data.

2.6 Estimation

The measured differential phase $\Phi_{D\text{-}InSAR}$ is composed of contributions from the uncompensated topography Φ_{herr}, of the displacement Φ_{displ}, of the atmosphere Φ_{atmo}, of the orbit Φ_{orbit} and of noise Φ_{noise}:

$$\varphi_{D-InSAR} = \varphi_{h_{err}} + \varphi_{displ} + \varphi_{atmo} + \varphi_{orbit} + \varphi_{noise} \,. \qquad (2)$$

Because the phase is measured modulo 2π a non-linear inversion problem is given. It is solved by utilising the different behaviour of the contributions regarding the acquisition parameters effective baseline, temporal baseline, range and azimuth location of the scatterers. Figure 2 visualises the different spatial properties for a subsidence, for an orbit error, for the atmosphere and for noise. A relative estimation between point scatterers located closely to each other reduces the influence of the atmosphere and of orbit errors. Utilising a periodogram a constant relative subsidence rate can be estimated. These relative estimates are transformed into a global subsidence map by a 2-D integration procedure based on a LS-adjustment.

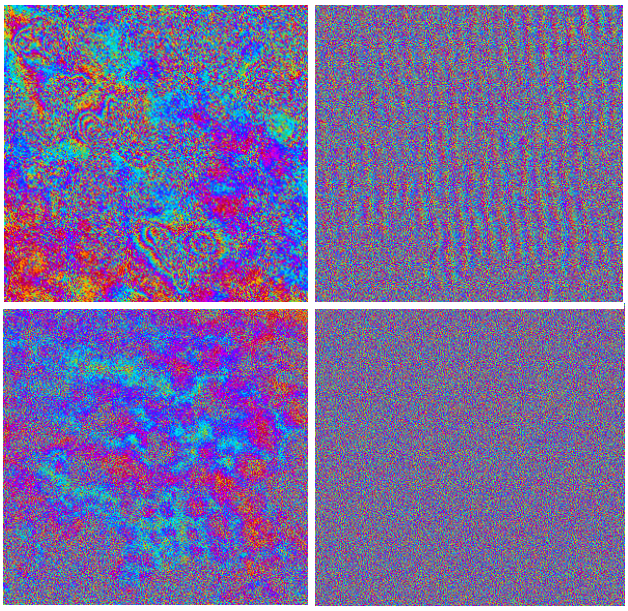

Figure 2. Visualisation of the different spatial behaviour of some contributions to the differential phase; upper left: subsidence; upper right: orbit error; lower left: atmospheric delay; lower right: noise; Additionally, the estimation utilises the properties regarding the effective and temporal baseline.

3. ADAPTED ALGORITHMS

This section presents two algorithms which needed to be adapted for the PS processing.

3.1 Co-registration

The co-registration is one of the most important processing steps in interferometry. For distributed scatterers, a co-registration inaccuracy introduces substantial noise into the interferometric phase (Bamler et al., 1993). And point scatterers have to deal with a systematic phase error (Holzner et al., 2001). With the PS interferometry, the co-registration becomes more difficult. The reason is the long time separation (up to ten years) between the acquisitions and the immense temporal decorrelation in non-urban areas. Figure 3 visualises the effect. Bamler (2000) showed that the error of the co-registration parameter estimation for distributed scatterer depends on the number of correlation points N and the coherence γ:

$$\sigma_{\Delta\hat{x}} = \sqrt{\frac{3}{2 \cdot N}} \cdot \frac{\sqrt{1-\gamma^2}}{\pi \cdot \gamma} \qquad (3)$$

in units of the resolution cell. Accordingly, in order to guarantee an appropriate co-registration accuracy in low

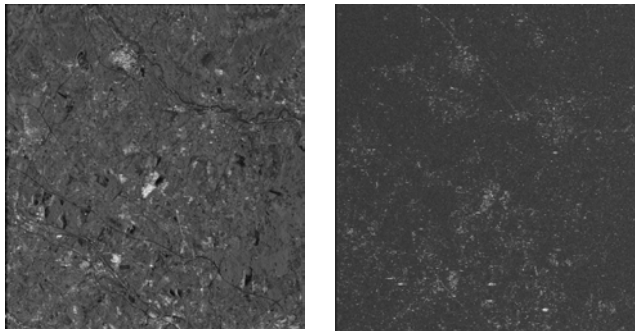

Figure 3. left image: scenes' intensity; right image: corresponding coherence. Obviously, urban areas and long time coherent areas correspond to each other. Consequently, only a few correlation points are left in order to co-register this scene and a regular correlation-based co-registration fails.

coherence scenes the correlation window size needs to be increased. However, the co-registration still strongly depends on the temporal coherence and the co-registration limit (Eq. 3) is often insufficient.

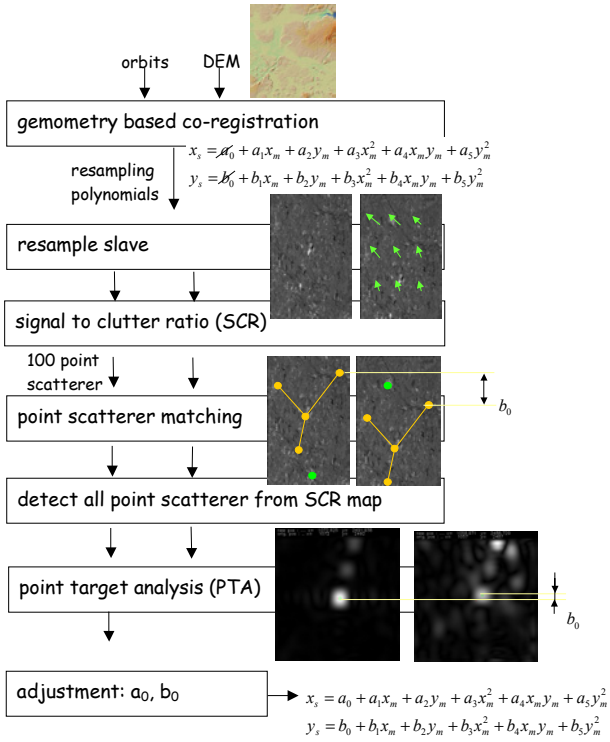

Figure 4. Principle of the newly developed robust geometry based co-registration

The newly developed co-registration module offers an accuracy independent of the scene coherence. Figure 4 visualises the principle of the algorithm. Correlation of SLC data is completely avoided. The basis is the availability of precise orbits and of a DEM. Both allow to simulate the observation geometry and consequently the transformation of the slave into the master scene. The scenes' transformation in range and azimuth is described by polynomials:

$$\begin{aligned} x_s &= a_0 + a_1x_m + a_2y_m + a_3x_m^2 + a_4x_my_m + a_5y_m^2 \\ y_s &= b_0 + b_1x_m + b_2y_m + b_3x_m^2 + b_4x_my_m + b_5y_m^2 \end{aligned} \qquad (4)$$

The time annotation in range and azimuth of some scenes can be incorrect. Therefore, the offset coefficients a_0 and b_0 are additionally estimated from SLC data. The coefficients a_0 and b_0 are initially set to zero and the slave scene is transformed using these polynomials into an approximate master geometry. Now, a half-pixel accurate shift of both scenes is determined. Based on the SCR the 100 most prominent point scatterers are detected. Assuming that these scatterers correspond to man-made features their spatial arrangement is matched with a huge search window of ±2000 samples in azimuth which corresponds to more than ±1 second timing error and ±500 samples in range. Because only 100 samples are involved this matching proceeds very fast. The coarse half-pixel accuracy is sufficient to position the point target analysis (PTA) window around each point scatterer and to initialise the starting position for the point scatterer peak detection. The accurate sub-pixel shift of both scenes is now determined by a PTA. Additionally, some quality measurements are computed in order to remove unsuitable point scatterers. Within the final processing step the coefficients of the geometry based estimation and of the offsets from the PTA are combined in a least squares adjustment. The adjustment only affects the low order polynomial coefficients. The reason is that the higher order coefficients are better determined by the precise orbits. An orbit error of 4 cm results in approximately 1/500 sample coregistration accuracy. The coefficient a_0 and b_0 correct for the timing. Additionally, the coefficients a_1, a_2, b_1 and b_2 can cope with diverging orbit errors.

3.2 Height-to-Phase Conversion

Within the PS processing one needs to know the height-to-phase conversion parameter exactly for each point. The reason is that the DEM update estimation utilises this factor B in the baseline-time diagram:

$$\phi_{insar} = \frac{4 \cdot \pi}{\lambda} \cdot \frac{B_N}{r \cdot \sin(\theta)} \cdot h_{topo} = B \cdot h_{topo} \qquad (5)$$

This equation indicates that the transformation of a scatterer height h_{topo} into a phase ϕ_{insar} depends on the look angle θ and the range distance r and consequently on the position of the scatterer in the scene. Figure 5 illustrates this fact. The crosses correspond to the location of the phase measurements in the periodogram estimation. Comparing the black crosses which indicate the scene centre conversion factor and the exact values which are highlighted in red color it becomes visible that the periodogram data changes. Actually, a scaling in the axis of ordinates takes place causing a height estimation bias. Consequently, the location of the data samples in the baseline-time diagram is updated at each PS position. The height-to-phase conversion factor is estimated numerically using the precise orbits and the mean topography height.

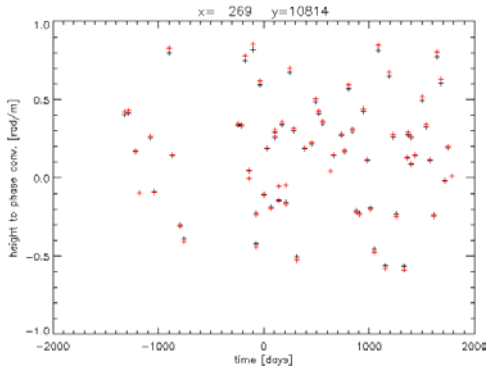

Figure 5. Change of the baseline-time diagram. Red crosses indicate the accurate and black crosses the scene centre height-to-phase-conversion factor.

4. DATA PRODUCTS

Apart from the standard interferometry data products like the interferogram and the coherence, the PS processing results in numerous new measurements offering a wide range of geophysical applications. Output are a displacement map, the evolution of each single scatterer in time, a DEM update at the PS locations and an atmospheric delay map. Some intermediate data are interesting as well for a further analysis. With the calibration a stack of co-registered σ^0 scenes results. This data stack can be used for classifications and for an extensive analysis of the point scatterer. By temporal power averaging of these data a radiometric improved multi-look (50-100) image of about optical quality can be generated, still offering the spatial resolution of the single input scenes. This high-quality radar image can be used for the visualisation of the estimates. Another application of the co-registered stack of SLC data with a wide span of baselines is the improvement of the resolution utilising the spectral shift (Rocca et al., 1993). This technique is implemented for the range direction. Figure 6 presents examples of the various data products from the developed PS processing system.

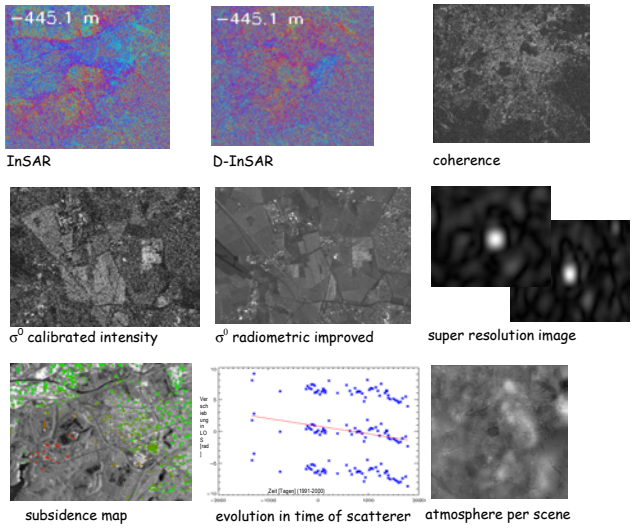

Figure 6. Examples for data products generated by the developed PS processing system.

5. APPLICATIONS

5.1 Test Site Bangkok

In the course of a Ph.D. work (Worawatanamateekul, 2003) an PS estimation has been computed for the city of Bangkok (Thailand). This test site causes some difficulties because only 17 ERS SLC scenes are available. Additionally, the test site is marked by a strong atmospheric signal contribution and an enormous subsidence rate. Figure 8 visualises the test site. The PS subsidence estimation (purple line) along the highlighted profile is compared with independent in situ measurements (blue line) in the upper right plot.

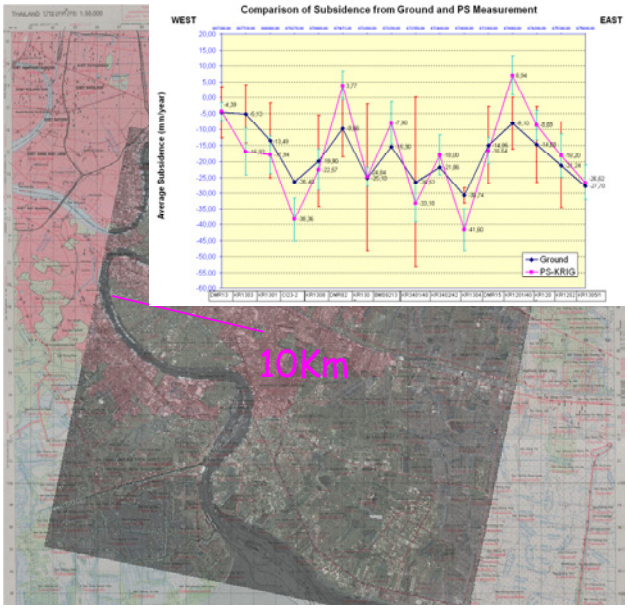

Figure 8. Test site Bangkok – the upper right plot shows the spatial profile through the subsidence: the purple color corresponds to the PS estimation, the blue color corresponds to independent in situ measurements.

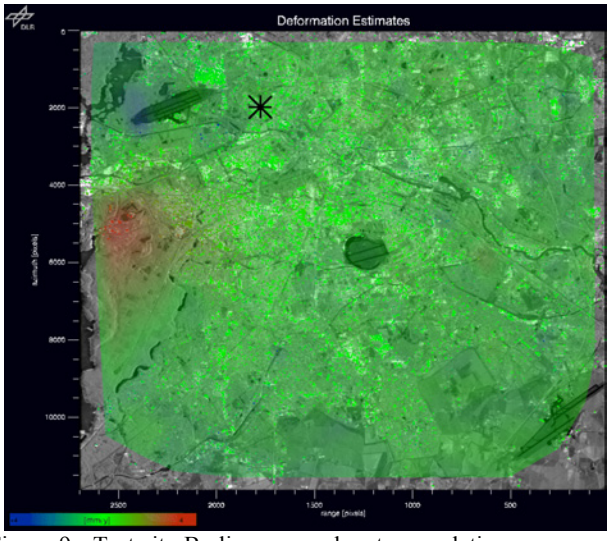

Figure 9. Test site Berlin – ground water regulation causes an uplift up to 3-4 mm per year (red area).

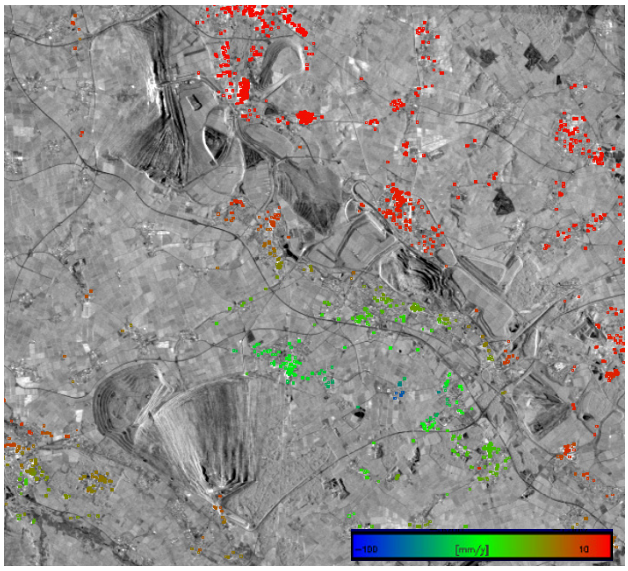

Figure 10. Test site Erft area – open cast mining area with subsidence up to 10 cm per year.

5.2 Test Site Berlin

The city of Berlin (Germany) is an agglomeration area with numerous huge construction sites. The red area in figure 9 results from ground water regulation. The mean displacement rate is approximately 3-4 mm per year. The data stack spans a time range of about ten years and consists of 70 scenes (Kampes et al., 2003).

5.3 Test Site Erft Area

In the open cast mining area around Bergheim, Hambach und Garzweiler (Germany) the ground water has been regulated. Figure 10 visualises the resulting subsidence. The difference between the red and the green dots corresponds to approximately 10 cm per year displacement. The data stack spans a time range of about 4 years. The high subsidence rate enables the comparison of the traditional D-InSAR technique and the PS processing (Kircher et al., 2003).

6. SUMMARY

The new data products of a permanent scatterer system enable numerous new geophysical applications. Consequently this innovative technique is implemented at DLR in a scientific processing system. Even with many years' experience developing radar interferometry software it is a challenging task because various practical obstacles needed to be overcome. The examples that result from our current application projects indicate that the scientific development and research system is becoming an operational tool for diverse applications.

7. ACKNOWLEDGEMENTS

ESA provided data for some test sites in the course of the projects ESA ITT No. AO 1-4124/02/NL/MM and ESA ITT No. AO/1-4231/02/I-LG. We gratefully acknowledge their support and the opportunity to participate in these projects.

8. REFERENCES

Bamler, R. and D. Just. 1993. Phase statistics and decorrelation in SAR interferograms. In: Proc. IGARSS 1993, 980-984.

Bamler, R. Interferometric Stereo Radargrammetry: Absolute Height Determination from ERS-ENVISAT Interferograms. In: Proc. IGARSS 2000, Honolulu, Hawaii, 24-28 July 2000, CDROM.

Bovenga F., A. Refice and R. Nutricato. 2002. Automated Calibration of Multi-temporal ERS SAR Data. In: Proc. IGARSS 2002, Toronto, Canada, 24-28 June 2002, CDROM.

Eineder, M. and N. Adam. A Flexible System for the Generation of Interferometric SAR Products, In: Proc. IGARSS 1997, Singapore, pp. 1341-1343, 1997.

Ferretti, A., C. Prati and F. Rocca. 1999a. Permanent Scatterers in SAR Interferometry. In: Proc. IGARSS 1999, Hamburg, Germany, 28 June-2 July 1999, 1528-1530.

Ferretti, A.; C. Prati and F. Rocca. 1999b. Non-Uniform Motion Monitoring Using the Permanent Scatterers Technique. In: Proc. FRINGE99, Liège, Belgium, http://earth.esa.int/pub/ESA_DOC/fringe1999.

Ferretti, A., C. Prati, F. Rocca and Politecnico di Milano. 2000a, Process for Radar Measurements of the Movements of City Areas and Labdsliding Zones. WO 00/72045 A1.

Ferretti, A., C. Prati. and F. Rocca. 2000b. Analysis of Permanent Scatterers in SAR Interferometry. In: Proc. IGARSS 2000, 24-28 July 2000, Honolulu, Hawaii, CDROM.

Ferretti A., F. Ferrucci, C. Prati and F. Rocca. 2000c. SAR Analysis of Building Collapse by Means of the Permanent Scatterers Technique. In: Proc. IGARSS 2000, Honolulu, Hawaii, 24-28 July 2000, CDROM.

Ferretti, A., C. Prati, and F. Rocca. 2000d. Measuring Subsidence with SAR Interferometry: Applications of the Permanent Scatterers Techniques. In: Proc. Sixth International Symposium on Land Subsidence, Vol. 2, Ravenna, 24-29 September 2000, 67-79.

Ferretti, A., C. Prati, and F. Rocca. 2000e. Nonlinear Subsidence Rate Estimation Using Permanent Scatterers in Differential SAR Interferometry. IEEE TGARS, Vol. 38, No. 5, September 2000, 2202-2212.

Ferretti, A., C. Prati, and F. Rocca. 2001. Permanent Scatteres in SAR Interferometry. IEEE TGARS, Vol. 39, No. 1, January 2001, 8-20.

Gatelli, F., A. M. Guarnieri, F. Parizzi, P. Pasquali, C. Prati, and F. Rocca. 1994. The Wavenumber Shift in SAR Interferometry. IEEE TGARS, Vol. 32, 855-865.

Holzner, J., S. Suchandt, M. Eineder, H. Breit and N. Adam. 2001. Co-registration - Geometrical Analysis and Verification for SAR Interferometry Under SRTM Data Conditions. In: Proc. IGARSS 2001, 9-13 July 2001, Sydney, CDROM

Kampes, B.M. and N. Adam. 2003. Velocity field retrieval from long-term coherent points in radar interferometric stacks. In: Proc. IGARSS 2003, Toulouse, CDROM.

Kircher, M., A. Roth, N. Adam, B. Kampes and H.J. Neugebauer. 2003. Remote Sensing Observation of Mining Induced Subsidence by means of differential SAR-Interferometry. In: Proc. IGARSS 2003, Toulouse, CDROM.

Laur H., P. Bally, P. Meadows, J. Sanchez, B. Schättler, E. Lopinto and D. Esteban. 2002. Derivation of the Backscattering Coefficient σ^0 in ERS SAR PRI Products. Document No. ES-TN-RS-PM-HL09, http://earth.esa.int/ESC2.

Nutricato, R., F. Bovenga and A. Refice. Optimum interpolation and resampling for PSC identification. In: Proc. IGARSS 2002, Toronto, Canada, 24-28 June 2002, CDROM.

Meadows, P. and B. Rosich. 2001. The ERS-2 SAR Performance: A Further Update. CEOS WGCV-SAR WORKSHOP 2001, Tokyo, Japan, 2-5 April 2001.

Prati, C. and F. Rocca. 1993. Improving Slant-Range Resolution with Multiple SAR Surveys. IEEE Transactions on Aerospace and Electronic Systems, Volume: 29 Issue: 1, Jan. 1993, 135 –144.

Usai S. and R. Klees. 1999. SAR Interferometry on Very Long Time Scale: A Study of the Interferometric Characteristics of Man-Made Features. IEEE Transactions on Geoscience and Remote Sensing, Vol. 37, No. 4, 2118-2123.

Worawatanamateekul, Jirathana. 2003. Ph.D. Thesis, to be submitted